

## COMPUTATIONAL STUDY OF DIFFUSIVITIES IN DIAMOND Ge-Si ALLOYS

S.L. Cui<sup>\*</sup>, L.J. Zhang<sup>\*\*</sup>, W.B. Zhang<sup>\*</sup>, Y. Du<sup>\*,#</sup>, H.H. Xu<sup>\*</sup>

<sup>\*</sup> State Key Laboratory of Powder Metallurgy, Central South University, Changsha, Hunan, 410083, PR China

<sup>\*\*</sup> Interdisciplinary Centre for Advanced Materials Simulation (ICAMS), Ruhr-Universität Bochum, 44801 Bochum, Germany

*(Received 02 November 2011; accepted 03 February 2012)*

---

### Abstract

*A variety of diffusivities in Ge-Si alloys available in the literature were critically reviewed. On the basis of the critically reviewed literature data, the diffusion parameters for self diffusivities and impurity diffusivities in diamond Ge-Si alloys were determined by considering the diffusion mechanism. A phenomenological treatment of the diffusivities in Ge-Si alloys were conducted. The finally obtained atomic mobilities can reproduce most of the diffusivities in diamond Ge-Si alloys as well as the concentration profiles of Ge-Si binary diffusion couples. In addition, the Manning modification on Darken Equation in diamond structure was also tested by using the presently obtained atomic mobilities.*

*Keywords: Ge-Si alloys; diffusion coefficients; atomic mobilities; Darken-Manning relation*

### 1. Introduction

Ge-Si alloys represent a very important type of semiconductor materials in microelectronic technology, and thus widely used as semiconductors in integrated circuits for heterojunction bipolar transistors, or as

high performance complementary metal oxide semiconductor (CMOS) applications [1]. Since the strained Si/SiGe heterostructures offer higher electron and hole mobilities than bulk Si, Ge-Si alloys have attracted extensive attention recently [2-3]. It is well known that the space

---

<sup>#</sup> Corresponding author: [yongducalphad@gmail.com](mailto:yongducalphad@gmail.com)

distributions of Ge, Si and possible dopants are of importance for the electrical behavior of SiGe-based device, which mainly depend on their diffusivity information. Moreover, diffusion coefficient is a determinant of the annealing time, the designated dimension of electronic device, and even the control of the charge carrier mobility and band structure of Si-Ge base electronic devices. Thus, a comprehensive knowledge of various diffusivities in solid Ge-Si alloys (diamond structure) is in urgent need if one wants to improve the electrical properties of SiGe-based device or even design new ones.

In order to acquire a full description of all kinds of diffusivities over the entire temperature and composition ranges, the recently developed DICTRA (DIffusion-CONTROLled TRANSformation) software in the framework of CALPHAD [4,5] (CALculation of PHase Diagram) method is an appropriate underlying tool to handle it. The so-called atomic mobility of each component is assessed based on a variety of reliable diffusivities, and stored in DICTRA type database, from which various diffusivities can be computed over the entire temperature and composition ranges, and various phase transformation processes can be simulated. The quality of atomic mobility strongly depends on the amount and the reliability of diffusivities. Though a certain amount of experimental diffusivities are available in the literature for diamond-structured Ge-Si alloys, the experimental data from different sources are usually not mutually consistent with each other. With the newly developed experimental techniques, such as secondary ion mass spectrometry (SIMS) [6], Raman spectroscopy [7], etc.,

more reliable experimental data are now available and the diffusivity measurement has been extended to low temperature. Therefore, a critical evaluation of all the available experimental diffusivities and their measurement techniques is necessary. Meanwhile, there exists only two pieces of information on assessment of atomic mobility in systems with diamond structure (only for pure Si by Zhang et al. [8] and Tang et al. [9]). Besides, whether the Darken equation or the Darken-Manning equation is applicable in systems with diamond structure still needs validation.

Consequently, the major aims of the present work are: (i) to critically review all the available diffusivities in Ge-Si alloys with diamond structure, (ii) to assess the atomic mobilities of Ge and Si in diamond-structured Ge-Si alloys based on the critically reviewed diffusivities, (iii) to validate both Darken and Darken-Manning equations in diamond Ge-Si alloys, and (iv) to verify the presently obtained atomic mobilities by comparing the simulated diffusion profiles with the experimental ones in Ge-Si thin film diffusion couples.

## 2. Models for diffusivities

Diffusion in Ge-Si alloys is mediated by the migration of intrinsic point defects, such as vacancies and interstitials. It is generally accepted that both vacancies and interstitials take part in the diffusion process in Si [7]. On the other hand, vacancy mechanism prevails over the whole temperature range for the self-diffusion in Ge [10]. There also exist evidences [6, 11] that the diffusion mechanism for Si diffusion in Ge follows the

diffusion mechanism of Ge self-diffusion, while that for Ge diffusion in Si follows the diffusion mechanism of Si self diffusion. According to Strohm et al. [6], the diffusion in Si<sub>y</sub>Ge<sub>1-y</sub> alloys is mediated by vacancies for 0<y<0.65, while for 0.65<y<1, either interstitial or vacancy plays a pivotal role in the diffusion process in SiGe alloys. As both vacancy and interstitial (neglecting other mechanisms, e.g. the direct exchange mechanism) may contribute to the self diffusion process, self or tracer diffusion coefficients can be written as [12]:

$$D^s = D_I^T + D_V^T = f_I D_I C_I^{eq} + f_V D_V C_V^{eq} \quad (1)$$

where  $D_X^T$  ( $X=I$  or  $V$ ) represents a contribution of the interstitialcy or vacancy to tracer diffusivities.  $f_X$  ( $X=I$  or  $V$ ) is the correlation factor for interstitialcy- or vacancy-mediated diffusion in diamond structure.  $f_V$  equals to 0.5 [13] for vacancy mechanism according to statistical diffusion theory and 0.53 or 0.46 [14] to atomistic study. While  $f_I$  is 0.73 (statistical diffusion theory) [15] and 0.59 or 0.69 (atomistic study) [14].  $C_X^{eq}$  and  $D_X$  ( $X=I$  or  $V$ ) are the equilibrium concentration and the diffusion coefficients of interstitialcy or vacancy, respectively. Intrinsic diffusivities correlates to tracer diffusivities by [16]:

$$D_A^I = D_A^T \left( 1 + \frac{\partial \ln \gamma_A}{\partial \ln x_A} \right) (1 + V_A) = D_A^T \Phi (1 + V_A) \quad (2)$$

and

$$V_A = \frac{2x_A}{M_0} \left( \frac{D_A^T - D_B^T}{x_A D_A^T + x_B D_B^T} \right) \quad (3)$$

where  $x_A$  is molar fraction of  $A$ ,  $\gamma_A$  is the activity coefficient of  $A$  and  $M_0$  is a constant for diamond structure, and equals to 2 [16].  $\Phi$  is thermodynamic factor and  $(1 + V_A)$  is the so

called ‘vacancy wind term’.

Manning corrected the Darken relation which relates the tracer and the chemical diffusivities by the vacancy wind factor  $S$  [16]:

$$\tilde{D} = (x_B D_A^T + x_A D_B^T) \Phi S \quad (4)$$

where  $S$  is given by

$$S = 1 + \frac{2x_A x_B (D_A^T - D_B^T)^2}{M_0 (x_A D_B^T + x_B D_A^T) (x_A D_A^T + x_B D_B^T)} \quad (5)$$

According to Andersson and Ågren [17], the atomic mobility of element  $B$ ,  $M_B$ , can be expressed as:

$$M_B = M_B^0 \exp\left(\frac{-Q_B}{RT}\right) \frac{1}{RT} {}^{mg}\Omega \quad (6)$$

where  $M_B^0$  is the frequency factor,  $Q_B$  the activation enthalpy,  $R$  the gas constant,  $T$  the temperature in Kelvin and  ${}^{mg}\Omega$  a factor taking into account the effect of ferromagnetic contribution to the diffusivities. For diamond structure the ferromagnetic contribution can be neglected, and then the atomic mobility parameters in the DICTRA [18] notation,  $Q_B$  and  $RT \ln M_B^0$ , can be grouped into one parameter, i.e.  $\Delta G_B$ . The composition dependency of  $\Delta G_B$  can be represented with the Redlich-Kister polynomial [19]:

$$\Delta G_B = \sum_i x_i \Delta G_B^i + \sum_i \sum_{j>i} x_i x_j \left[ \sum_{r=0,1,\dots}^n {}^r \Delta G_B^{i,j} (x_i - x_j)^r \right] \quad (7)$$

where  $\Delta G_B^i$  is the value of  $\Delta G_B$  for  $B$  in pure  $i$ , while  ${}^r \Delta G_B^{i,j}$  are the binary interaction parameters.

The tracer diffusivities  $D_i^T$  relates to the atomic mobilities via the Einstein relation:  $D_i^T = RT M_i$ . Neglecting Manning correction, the interdiffusion coefficients defined with  $n$  as solvent are correlated to the atomic mobilities by [17]:

$$\tilde{D}_{kj}^n = \sum_i (\delta_{ik} - x_k) x_i M_i \left( \frac{\partial \mu_i}{\partial x_j} - \frac{\partial \mu_i}{\partial x_n} \right) \quad (8)$$

where  $\delta_{ik}$  is the Kroneker delta (  $\delta_{ik} = 1$ , if  $i = j$ , otherwise  $\delta_{ik} = 0$  ) and  $\mu_i$  is the chemical potential of element  $i$ .

### 3. Review of literature data

In light of the technical importance of Ge-Si alloys in semiconductor industry, a host of experimental investigations were conducted for the sake of the understanding of its kinetic properties, including diffusion mechanism, atomic transportation velocity, the contribution of each type of diffusion mechanisms towards diffusion coefficients, etc. As a result, there exist

a considerable large amount of experimental diffusivities in the literature, which can be categorized into self diffusivities, impurity diffusivities, tracer diffusivities and interdiffusivities.

#### 3.1 Self diffusivities of Si

Two types of self diffusivities data are considered in the present work. One is those measured using direct self-diffusion measurement, while the other is the self diffusivities determined via metal diffusion experiments. A summary of these data are listed in **Table 1**, and concisely presented as follows.

Table 1 Summary of experimentally measured self diffusivities of Si

Data type	Temperature range (K)	Method <sup>a</sup>	Ref.	Code <sup>b</sup>
Self diffusivity of Si	1373-1573	<sup>31</sup> Si tracer, single crystal	[20]	+
	1451-1573	<sup>30</sup> Si tracer, single crystal	[21]	+
	1473-1673	<sup>31</sup> Si tracer	[22]	□
	1373-1573	<sup>31</sup> Si tracer, single crystal	[23]	□
	1243-1343	LAT	[24]	+
	1593-1873	SST	[25]	+
	1173-1373	(p, $\gamma$ ) RBM	[26]	+
	1273-1523	RMT	[27]	□
	1258-1448	<sup>30</sup> Si, IAT	[28]	□
	1203-1473	ion implantation <sup>30</sup> Si, (p, $\gamma$ ) RA	[29]	□
	1128-1661	isotopically enriched <sup>28</sup> Si, SIMS	[30]	■
	1073-1373	isotopically enriched <sup>30</sup> Si, SIMS	[31, 32]	■
		<sup>31</sup> Si, IGISOT, SIMS, single crystal	[6]	■
	1143-1343	isotopically enriched <sup>30</sup> Si, SIMS	[33, 34]	■
	1146-1573	isotopically enriched <sup>30</sup> Si, SIMS	[35]	■
908-1148	Roman spectroscopy	[7, 36]	■	
Interstitialcy component	1073-1371	Au in Si, NAA, MS, SRT	[37]	■
	973-1073	Pt in Si, DTS, DCBM	[38]	□
	1262	Zn in Si, SRT	[39]	■
	1175-1473	Zn in Si, NAA, SRT	[40]	□
	1273-1573	Pt in Si, NAA, MS, SRT	[41]	■
	1143-1148	Zn in Si, NAA, MS, SRT	[12]	■

<sup>a</sup> LAT=the loop annealing technique, SST=the sputter-sectioning technique, (p,  $\gamma$ ) RBM=the (p,  $\gamma$ ) resonance broadening method, RMT=radioisotope microsectioning technique, IAT=radioisotope microsectioning technique, (p,  $\gamma$ ) RA=(p,  $\gamma$ ) reaction analysis, SIMS=secondary ion mass spectrometry, IGISOT=the ion guide isotope separator on-line technique, NAA=the neutron activation analysis, MS=mechanical sectioning, SRT=the spreading resistance technique, DTS=the deep-level transient spectroscopy, DCBM=diode capacitance/reverse bias measurements. <sup>b</sup> Indicates whether the data are used or not used in the atomic mobility assessment: ■, used; □, used but with low weight; +, not used but considered as reliable data.

The former group contains various contributions. Master and Fairfield [20] investigated the self diffusivities of  $^{31}\text{Si}$  in single crystal Si between 1373 K and 1573 K via the determination of the concentration profile by an anodization-etching technique combined with liquid scintillation radioassay. Using evaporated  $^{30}\text{Si}$  source, the self diffusivities of Si at 1451 and 1573 K were determined by Ghoshtagore [21] in p- and n-type single crystals Si using chemical sectioning. Si self diffusivities in intrinsic Si were investigated by Peart [22] using the radio isotope  $^{31}\text{Si}$  as tracer in the temperature range of 1473 to 1673 K. Just after that, Fairfield and Masters [23] studied the diffusion of  $^{31}\text{Si}$  into Si single crystals within the range of 1373 and 1573 K and mono-vacancy mechanism was proposed for Si self diffusion. The loop annealing technique was applied to the study of self diffusion in silicon over a wide range of temperature from 1243 to 1343 K by Sanders and Dobson [24], who found that the diffusion coefficients decreases as the concentration of n-type dopant decreases and the concentration of p-type dopant increases. With the aid of a sputter-sectioning technique, Mayer et al. [25] determined the self-diffusion coefficients in high purity p-type Si at 1593-1873 K. The (p,  $\gamma$ ) resonance broadening method was utilized by Hirvonen and Anttila [26] to measure the self diffusivities of Si in the temperature range of 1173 and 1373 K. At the meantime, self diffusivities of Si in intrinsic and doped Si were investigated by Hettich et al. [27] via radiotracer microsectioning techniques. Kalinowski and Seguin [28] investigated the self diffusivities of  $^{30}\text{Si}$  in intrinsic Si by

means of an ion-analyzer technique and obtained the temperature dependence of the diffusion coefficients in the range from 1258 to 1448 K. By using the ion implantation for preparation and (p,  $\gamma$ ) reaction for analysis of  $^{30}\text{Si}$  profiles, the Si self diffusion was studied in the temperature range of 1203 and 1473 K by Demond et al. [29]. Bracht et al. [30] measured the self diffusion of silicon in highly isotopically enriched  $^{28}\text{Si}$  layers between 1128 and 1661 K with the profiles of  $^{29}\text{Si}$  and  $^{30}\text{Si}$  determined by SIMS. Their experiments indicate that self interstitials dominate the Si self diffusion process. Ural et al. [31, 32] conducted experimental investigation on the self diffusivities of Si using epitaxially grown isotopically enriched Si and SIMS technique in the temperature range between 1073 and 1373 K. Strohm et al. [6] utilized the  $^{31}\text{Si}$  ions produced by the ion guide isotope separator on-line technique to measure the self diffusivities of Si single crystal. By using isotopically pure  $^{30}\text{Si}$  epitaxial layers as a diffusion source to bulk Si substrates coupled with SIMS technique, Nakabayashi et al. [33, 34] obtained the Si self diffusion coefficients in intrinsic single crystal bulk Si at 1143-1343 K. Using the highly isotopically enriched  $^{30}\text{Si}$  epitaxial layers as a diffusion source to bulk and epitaxial layers Si, with the concentration profiles determined by SIMS, Aid et al. [35] determined the diffusivities of  $^{30}\text{Si}$  in the temperature range of 1146-1573 K. Shimizu et al. [7, 36] overcame the handicap of SIMS in measuring the diffusivities of Si at low temperature by detection of the very small diffusion length in isotope super-lattices of Si via Raman spectroscopy. Their determined self diffusion coefficients of Si at

temperatures 908-1148 K show low activation energy of 3.6 eV which is lower than that of the high temperature data and in agreement with the theoretical prediction for the vacancy mediated diffusion.

Another type of self diffusivities measurement is based on metal elements which diffuse in Si mainly via kick-out mechanism. Stolwijk et al. [37] investigated the in- and out- diffusion of Au in Si by means of a neutron activation analysis combined with mechanical sectioning or by the spreading resistance technique. The interstitialcy contribution to the Si self-diffusion coefficient was determined at the temperature range of 1073-1371 K from the Au solubility and diffusion measurement. By utilizing the deep-level transient spectroscopy and diode capacitance/reverse bias measurements, the in-diffusion of Pt in n-type Si from a platinum silicide source was investigated by Mantovani et al. [38] at 973-1073 K. The result indicated that the Pt diffusion in Si via kick out mechanism, while the self diffusion of Si mainly via interstitialcy mechanism at the experimental temperature range. Perrett et al. [39] studied the interstitialcy contribution of Si self diffusion via measurement of the kick out type diffusion of Zn in Si at 1262 K. Subsequently, Grünebaum et al. [40] conducted experimental investigations of Zn diffusion in dislocation free and plastically deformed Si with the same measurement techniques. They further verified the kick-out mechanism of Zn diffusion in Si and determined the interstitialcy diffusivities of Si at 1175-1473 K. Likewise, Hauber et al. [41] derived the interstitialcy component of Si self diffusivities between 1273 and 1573

K by measurement of diffusivities and solubility of Pt in dislocation-free Si using both neutron-activation analysis in combination with mechanical serial sectioning and spreading-resistance measurement. With similar approach, Bracht et al. [12] investigated the diffusion of Zn in dislocation free Si between 1143 and 1481 K and obtained the interstitialcy component of Si self diffusivities.

### 3.2 Self-diffusivities of Ge

In contrast to Si, Ge has more stable radioisotope, i.e.  $^{71}\text{Ge}$ . The self diffusion measurement using the radioactive tracer method is much more applicable with respect to Si. As a result, the available experimental data from different sources are generally in good agreement. A brief summary of these data are listed in **Table 2**. Letaw et al. [42, 43] reported two pieces of information on the self diffusivities in Ge using  $^{71}\text{Ge}$  as tracer. Their data cover the temperature range from 1039 to 1201 K. Valenta and Ramasastry [44] determined the self diffusivities of Ge for intrinsic n-type and p-type single crystal Ge at various temperatures by utilizing  $^{61}\text{Ge}$ . Widmer and Gunther-Mohr [45] measured the Ge self diffusivities in the temperature range of 993 to 1027 K by way of a residual activity technique with radioactive  $^{71}\text{Ge}$  as tracer. Subsequently, Widmer [46] studied the  $^{71}\text{Ge}$  diffusion in intrinsic Ge single crystals at the temperature near 1013 K using the same measurement method. Campbell [47] performed experimental investigation of Ge self diffusion by simultaneously diffusing the isotopes  $^{77}\text{Ge}$  and  $^{71}\text{Ge}$  into single crystal intrinsic Ge at 1173 and 1198 K with a

sectioning and counting method. Using  $^{71}\text{Ge}$  as radioisotope and a sputtering technique for serial sectioning, Vogel et al. [48] investigated the self diffusivities in intrinsic Ge single crystals in the temperature range of 822-1163 K. The tracer diffusion coefficients for  $^{71}\text{Ge}$  were measured in Ge single crystals as a function of pressure, temperature, and doping in the temperature range of 808-1177 K by Werner and Mehrer [49] with the ion beam sputtering for microsectioning. By using isotope heterostructures  $^{70}\text{Ge}$  and  $^{74}\text{Ge}$  as tracer, with SIMS measured the diffusion profiles; Fuchs et al. [50, 51] determined the self diffusivities of Ge at the temperature range of 816 to 913 K. Silveira et al. [52] studied the self diffusion of Ge using the Roman scattering by optical phonons in

isotopic  $(^{70}\text{Ge})_n(^{74}\text{Ge})_m$  super-lattices at 773 K. The obtained diffusion coefficient agrees well with that from the previously reported ones. Almazouzi et al. [53] determined the bulk and grain boundary diffusion of Ge in Ge using radioactive  $^{68}\text{Ge}$  as tracer in conjunction with mechanical sectioning at several temperatures. Strohm et al. [6, 54] conducted two pieces of experiments in the measurement of the self diffusion coefficients in single crystals Ge. The self diffusivities of  $^{71}\text{Ge}$  in relaxed Ge epitaxial layers were measured at 1167 to 1536 K by means of a radioactive technique combined with ion beam sputtering. By neutron reflectometry from the decay of the first and third order Bragg peak, Hüger et al. [10] investigated the self diffusion in intrinsic

Table 2 Summary of experimentally measured self diffusivities of Ge

Data type	Temperature range (K)	Method <sup>a</sup>	Ref.	Code <sup>b</sup>
Self diffusivity of Ge	1039-1210	$^{71}\text{Ge}$ tracer	[42, 43]	□
	1023-1173	$^{61}\text{Ge}$ tracer, single crystal	[44]	■
	993-1027	$^{71}\text{Ge}$ tracer, RAT	[45]	□
	~1013	$^{71}\text{Ge}$ tracer, RAT	[46]	■
	1173-1198	$^{77}\text{Ge}$ , $^{71}\text{Ge}$ tracer, SCM, single crystal	[47]	■
	822-1163	$^{71}\text{Ge}$ tracer, SCM, single crystal	[48]	■
	808-1173	$^{71}\text{Ge}$ tracer, IBSM, single crystal	[49]	■
	816-913	$^{70}\text{Ge}$ , $^{74}\text{Ge}$ tracer, SIMS	[50, 51]	■
	773	Roman scattering measurement	[52]	■
	910-1023	$^{68}\text{Ge}$ tracer, mechanical sectioning	[53]	+
	1167-1536	$^{71}\text{Ge}$ tracer, IBSM, single crystal	[6, 54]	■
	702-869	$^{70}\text{Ge}/^{\text{nat}}\text{Ge}$ isotope, single crystal	[10]	■
	813-1123	implanted $^{71}\text{Ge}$ tracer	[55]	■
	850-1200	Cu in Ge, SRT	[56]	+

<sup>a</sup> RAT=the residual activity technique, SCM=the sectioning and counting method, IBSM=the ion beam sputtering for microsectioning, SIMS=secondary ion mass spectrometry, SRT=the spreading resistance technique. <sup>b</sup> Indicates whether the data are used or not used in the atomic mobility assessment: ■, used; □, used but with low weight;+, not used but considered as reliable data.

single crystalline Ge between 702 and 869 K using  $^{70}\text{Ge}/^{nat}\text{Ge}$  isotope multilayer structures. Single vacancies were considered as the main diffusion mechanism in Ge over the whole temperature range. Laitinen et al. [55] studied the self diffusion coefficients implanted  $^{71}\text{Ge}$  in bulk Ge at the temperature range 813-1123 K by means of a modified radiotracer technique. By measurement of the diffusion profiles and the solubility of Cu in Ge via the spreading resistance technique, self diffusivities of Ge were calculated between 850 and 1200 K by Stolwijk et al. [56].

### 3.3 Impurity diffusivities of Ge in Si

Several groups of authors contribute to the measurement of the diffusion coefficients of Ge in Si as summarized in **Table 3**. Petrov et al. [57] obtained the diffusivities of  $^{71}\text{Ge}$  in polycrystalline p-type Si by way of a residual activity measurement method at 1423 to 1623 K. Subsequently, McVay and DuCharme [58] measured the diffusion of Ge in single crystalline Si by utilizing the radioactive tracer  $^{71}\text{Ge}$  and a thin sectioning technique at various temperatures. Impurity diffusivities of Ge in intrinsic and doped Si

Table 3 Summary of experimentally measured impurity diffusivities in Ge-Si alloys

Data type	Temperature range (K)	Method <sup>a</sup>	Ref.	Code <sup>b</sup>
Impurity diffusivity Ge	1423-1623	$^{71}\text{Ge}$ tracer, RAMM, polycrystal	[57]	+
	~1400-1700	$^{71}\text{Ge}$ tracer, TST, single crystal	[58]	■
	1273-1523	$^{71}\text{Ge}$ tracer, RMT	[27]	■
	1373-1573	SIMS	[59]	■
	1149-1661	SIMS	[60, 61]	■
	973-1223	Raman scattering, X-ray reflectometry	[62]	+
	1173-1323	SIMS	[63]	■
	873-1123	$^{71}\text{Ge}$ tracer, IBSM	[6, 54]	■
	1143-1543	SIMS	[64]	■
Impurity diffusivity Si	923-1173	$^{31}\text{Si}$ tracer, (p, $\gamma$ ) RBM	[65]	+
	973-1223	Raman scattering, X-ray reflectometry	[62]	□
	923-1203	SIMS	[66]	■
	1123-1273	$^{31}\text{Si}$ tracer, IGISOT, single crystal	[6]	■
	1023-1148	SIMS	[67]	■
	823-1173	SIMS	[11, 68]	■

<sup>a</sup> RAMM=the residual activity measurement methods, TST=the thin sectioning technique, RMT=the radiotracer microsectioning technique, IBSM=the ion beam sputtering for microsectioning, (p,  $\gamma$ )RBM=the (p,  $\gamma$ ) resonance broadening method, SIMS=secondary ion mass spectrometry, IGISOT=the ion guide isotope separator on-line technique. <sup>b</sup> Indicates whether the data are used or not used in the atomic mobility assessment: ■, used; □, used but with low weight; +, not used but considered as reliable data.



were investigated by Hettich et al. [27] via radiotracer microsectioning techniques. Their results indicated that the low temperature process was enhanced by As doping and lowed by B doping, while at high temperature the process was enhanced by both B and As doping. Interstitialcy and vacancy were considered as the diffusion mechanism of high temperature and low temperature respectively. Diffusivities of Ge in Si at the temperature range of 1373-1573 K were measured by Ogino et al. [59] using SIMS technique. Using 38 specimens, diffusion of Ge as a lattice impurity in Si was studied by Dorner et al. [60, 61] at temperatures between 1149 and 1661 K with the concentration profiles measured via SIMS. The Arrhenius plot of the diffusivities exhibited straight line which contradicted with the results obtained by Hettich et al. [27]. Lockwood et al. [62] investigated the diffusivities of Ge in Si from 973 to 1223 K by way of a Raman scattering and X-ray reflectometry study. Zangenberg et al. [63] determined the impurity diffusivities of Ge in Si in strain-relaxed Si by means of SIMS technique at 1173-1323 K. Meanwhile, Strohm et al. [6, 54] measured the impurity diffusivities of Ge in single crystalline Si by means of radiotracer techniques and serial sectioning done by ion beam sputtering between 873 and 1123 K. Recently, Kube et al. [64] conducted diffusion measurement using SIMS technique and determined the diffusivities of Ge in (110) oriented Si at the temperature range of 1143-1543 K.

### 3.4 Impurity diffusivities of Si in Ge

The available experimental measurements

of impurity diffusivities of Si in Ge are limited to Räsänen et al. [65], Lockwood et al. [62], Sodervall and Friesel [66], Strohm et al. [6], Uppal et al. [67] and Silverstri et al. [11, 68] ( also see **Table 3**). The impurity diffusivities of Si in Ge were firstly measured by Räsänen et al. [65] using  $^{31}\text{Si}$  as tracer in n-type and p-type Ge with the concentration profiles determined by the ( $\rho$ ,  $\gamma$ ) resonance broadening method in the temperature range from 923 to 1173 K. Lockwood et al. [62] investigated the diffusivities of Si in Ge from 973 to 1223 K by way of a Raman scattering and X-ray reflectometry study. Another piece of contribution is due to Sodervall and Friesel [66] who measured the diffusivities of Si in Ge via the concentration profiles analyzed by SIMS technique between 923 and 1203 K. Taking  $^{31}\text{Si}$  as radioactive tracer, ion beam sputtering for sectioning, Strohm et al. [6] investigated the impurity diffusivities of Si in single crystalline Ge at about 1123-1273 K. Employing the implantation doped Si as tracer, Uppal et al. [67] studied the diffusivities of Si in Ge at the temperature range from 1023 to 1148 K with the concentration profiles measured by SIMS technique. The result revealed an activation energy of  $3.2(\pm 0.3)$  eV for Si which is closer to that for Ge self diffusion, indicated that the diffusion mechanism of Si diffuse in Ge is the same as that of Ge self diffusion. Recently, by utilizing a molecular beam epitaxy (MBE) grown buried Si layer in an epitaxial Ge layer on a crystalline Ge substrate as the source of diffusion, Silvestri et al. [11, 68] measured the diffusion coefficients of Si in crystalline Ge over the temperature range of 823-1173 K aided with

SIMS technique. The obtained activation energy is  $(3.32 \pm 0.03)$  eV which also indicates a vacancy-mediated diffusion of Si in Ge.

### 3.5 Tracer diffusivities

A brief summary of the tracer diffusivities available in the literature is in **Table 4**. The measurement of the tracer diffusivities in Ge-Si alloys started from McVay and DuCharme [69] who determined the tracer diffusivities of  $^{71}\text{Ge}$  in polycrystalline Ge-Si alloys containing 22.4 at.% Ge, 30.8 at.% Ge, 55.4 at.% Ge and 77.7 at.% Ge. Their data revealed an abrupt decrease of the activation energy as the composition of Ge increases and reaches a platform at about 40

at.% Ge. More than three decades later, Zangenberg et al. [63] determined the diffusion coefficients and activation energies for  $^{72}\text{Ge}$  diffusion in strain relaxed  $\text{Si}_{1-x}\text{Ge}_x$  ( $x = 0.1, 0.2, 0.3, 0.4$  and  $0.5$ ) by means of SIMS technique in the temperature range of 1123 to 1323 K. According to their study, the activation energy for Ge diffusion is 4.7 eV for  $\text{Si}_{1-x}\text{Ge}_x$  alloys with  $x = 0 \sim 0.1$ , and 3.7 to 4.0 eV for alloys with  $x = 0.2 \sim 0.4$ . Strohm et al. [6, 54] also contributed to the measurement of tracer diffusivities in single crystalline Ge-Si alloys. The diffusivities of  $^{71}\text{Ge}$  were determined in a wide composition range of 923-1536 K via a radioactive technique coupled with ion beam sputtering. Similarly, the diffusivities of  $^{31}\text{Si}$  in  $\text{Si}_{1-x}\text{Ge}_x$  ( $x = 0.2$  and  $0.5$ ) alloys were measured. Their

Table 4 Summary of experimentally measured tracer and inter-diffusivities in Ge-Si alloys

Data type	Temperature range (K)	Method <sup>a</sup>	Ref.	Code <sup>b</sup>
Tracer diffusivity Ge	1004-1525	$^{71}\text{Ge}$ tracer, polycrystal	[69]	+
	1123-1323	$^{72}\text{Ge}$ tracer, SIMS	[63]	□
	923-1536	$^{71}\text{Ge}$ tracer, IBSM	[6, 54]	■
	813-1123	$^{71}\text{Ge}$ , MRT	[55]	■
	1143-1543	SIMS	[64]	■
Tracer diffusivity Si	~1100-1300	$^{31}\text{Si}$ , IGISOT, SIMS, single crystal	[6, 54]	■
	813-1123	$^{31}\text{Si}$ , MRT	[55]	■
	1143-1543	SIMS	[64]	■
Interdiffusivity	550-630	X-ray diffraction	[70]	+
	1043-1143	X-ray diffraction	[71]	♣
	1173-1398	Rutherford backscattering spectrometry	[72]	+
	1023-1173	BMM, SIMS	[73, 74]	+
	1043-1193	BMM	[75-77]	♣
	900-1100	X-ray specular reflectivity	[78-80]	♣
	873-973	X-ray reflectivity measurement	[81]	♣

<sup>a</sup> IBSM=the ion beam sputtering for microsectioning, MRT=the modified radioactive technique, SIMS=secondary ion mass spectrometry, BMM=Boltzmann-Matano method. <sup>b</sup> Indicates whether the data are used or not used in the atomic mobility assessment: ■, used; □, partially used; +, not used; ♣, not used but considered as reliable.

research indicated that the activation energies for  $^{71}\text{Ge}$  tracer diffusivities slightly decrease from 4.6 eV to approximately 4.25 eV firstly, and then shoot up to about 5.5 eV for Ge self diffusivities. This trend is in contradiction with that reported by McVay and DuCharme [69]. While the pre-exponential factors for  $^{71}\text{Ge}$  tracer diffusivities rise considerably from  $2 \times 10^{-4}$  to  $4 \times 10^{-2}$   $\text{m}^2/\text{s}$ . Tracer diffusivities of implanted  $^{31}\text{Si}$  and  $^{71}\text{Ge}$  in relaxed  $\text{Si}_{0.20}\text{Ge}_{0.80}$  layers were investigated by Laitinen et al. [55] in the temperature range of 813-1123 K by way of a modified radioactive technique. Experiments on the diffusion of Si and Ge in  $\text{Si}_{1-x}\text{Ge}_x$  ( $x = 0.05$  and  $0.25$ ) isotope heterostructures between 1143 and 1543 K were conducted by Kube et al. [64] with the concentration profiles determined by SIMS.

### 3.6 Inter-diffusivities

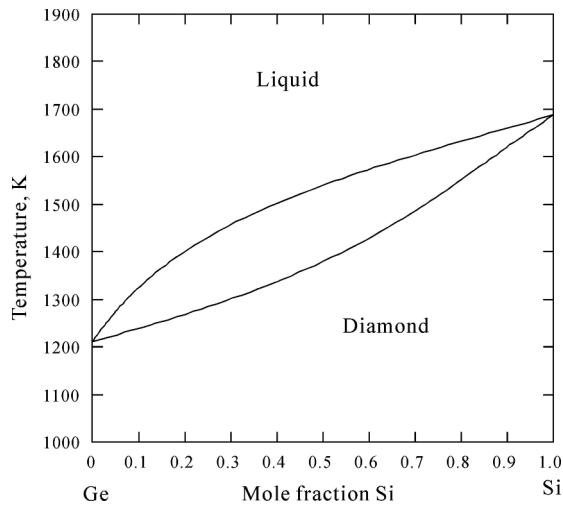
Early measurement of interdiffusion coefficients in Si/Ge amorphous multilayer films was conducted by Prokes and Spaepen [70] in the temperature range of 550-630 K. The interdiffusivities were determined by measuring the intensity of the X-ray satellite arising from the modulation as a function of annealing time. A systematically measurement of Ge-Si interdiffusivities for Ge concentration between 0.075 and 0.192 over the temperature range of 1043~1143 K was conducted by Aubertine and McIntyre [71]. Holländer et al. [72] studied the thermal interdiffusion in both asymmetrically and symmetrically strained  $\text{Si}/\text{Si}_{1-x}\text{Ge}_x$  superlattices with Ge concentration between  $x=0.2$  and  $0.70$  using Rutherford

backscattering spectrometry in the temperature range between 1173 to 1398 K. Recently, the interdiffusion coefficients were determined by Gavelle et al. [73, 74] using the Boltzmann-Matano method from the concentration profiles of Ge derived by SIMS measurement in the temperature range of 1023-1173 K. Xia et al. [75-77] derived the diffusion coefficients in epitaxial strained  $\text{Si}/\text{Si}_{1-y}\text{Ge}_y/\text{strained Si}/\text{relaxed Si}_{1-x0}\text{Ge}_{x0}$  heterostructures for Ge concentration between 0 and 0.56 over the temperature of 1043 to 1193 K by using the Boltzmann-Matano method. The concentration profiles were determined via SIMS technique. Meduña et al. [78-80] contributed to the measurement of interdiffusivities of GeSi alloys containing 0.25, 0.50, 0.70 and 0.90 at.% Ge by X-ray specular reflectivity using *ex-situ* and *in-situ* annealing experiments. Similarly, Ozguven and McIntyre [81] investigated the interdiffusion in epitaxial  $\text{Si}_x\text{Ge}_{1-x}/\text{Si}_y\text{Ge}_{1-y}$  superlattices that have an average Ge composition of 91 at. %. The interdiffusion information mentioned above is also summarized in **Table 4**.

### 4. Determination of diffusion parameters

Diffusion process in Ge-Si alloys is of significance for the fabrication of electronic devices. In order to understand the properties of point defect in Ge-Si alloy, it is necessary to determine the diffusion parameters for Ge-Si alloys. Here, the diffusion parameters for self diffusivities and impurity diffusivities were evaluated first. And then the tracer diffusivities were modeled by employing the model developed by Andersson and Ågren [17]. During the present modeling, the

thermodynamic description for Ge-Si binary system obtained by Bergman et al. [82] was utilized to calculate the thermodynamic factor. **Fig. 1** presents the calculated Ge-Si



phase diagram.

Figure 1. Calculated Ge-Si phase diagram due to the thermodynamic parameters obtained by Bergman et al. [82].

As discussed in section 3.1, there are two types of measurements for the self diffusivities of Si: direct measurement and metal experiment. Direct self diffusion measurement in Si cannot separate the relative contribution of interstitialcy mechanism and vacancy mechanism. Fortunately, this drawback can be compensated by metal diffusion experiment [12], because information about intrinsic point defects can also be obtained by studying foreign-atom diffusion in Si when the interstitialcy and/or vacancy are involved in the diffusion process. For example, mainly substitution dissolved foreign atoms, like group III and V elements, need vacancies and interstitials as vehicles for transportation in Si.

Experimental investigation indicated that diffusion of Zn [12, 39, 40], Au [37], and Pt [38, 41] in Si via kick-out mechanism. In these studies, the interstitialcy component of Si self diffusivities was determined. As a result, the self diffusivities of Si can be described using a double Arrhenius equation [83]. Firstly, the interstitialcy component of Si self diffusivities was determined by least square fit of experimental data obtained using metal experiment [12, 37-41]. One thing worth addressing is that the correlation factors used by different sources are quite different, i.e. Stolwijk et al. [37], Perrett et al. [39], Grünebaum et al. [40] and Hauber et al. [41] utilized 0.5, Mantovani et al. [38] used 0.99999, and Bracht et al. [12] used 0.73. For consistency, a correlation factor of 0.73 [15] was accepted and the experimental data were adjusted by this correlation factor. Then, the vacancy component was evaluated mainly using the direct measurement by SIMS from Bracht et al. [30], Ural et al. [31, 32], Strohm et al. [6], Aid et al. [35], Shimizu et al. [7, 36] and Nakabayashi et al. [33, 34]. While other data are not utilized or only with a low weight, this is due to the fact that  $^{31}\text{Si}$  has a half life of only about 2.6 h which limits the self diffusion studies to a rather narrow temperature and short annealing time or due to the Si samples used were doped. In addition, the experimental data from Master and Fairfield [20], Mayer et al. [25] and Hirvonen and Anttila [26] exhibit apparent divergence with others. The finally obtained diffusion parameter for Si self diffusivity is presented as:

$$D_{\text{Si}}^T = 0.37146010 \exp\left(\frac{-485572.27}{RT}\right) + 2.5433246 \times 10^{-7} \exp\left(\frac{-345475.76}{RT}\right) \text{ m}^2/\text{s} \quad (9)$$

where the first term is the interstitialcy component and second term is the vacancy component. **Fig. 2** presents the Arrhenius plot of Si self diffusivities together with the literature data. The solid line refers to the Si self diffusivities, while the dotted and dashed lines are the interstitialcy component and the vacancy component, respectively. It is apparent from the figure that interstitialcy mechanism dominates the diffusion process at high temperature, while vacancy mechanism is the main mechanism at low temperature. From Eq. 9, the activation energy for interstitialcy mechanism and vacancy mechanism are 5.04 eV and 3.59 eV which agree well with the theory value [84] 4-4.9 eV and 3.07-4.9 eV respectively.

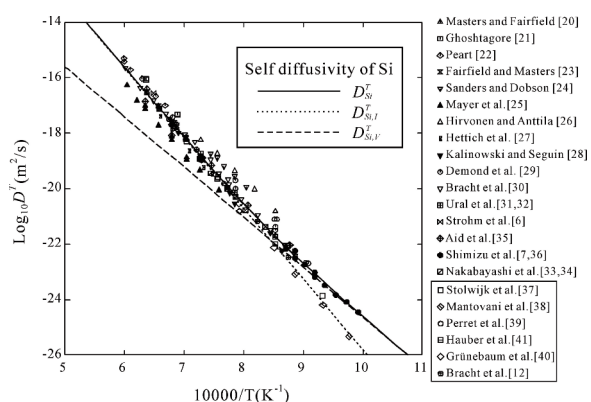


Figure 2. Self diffusivities of Si. All the lines are from the present evaluation: the solid line is the Si self diffusivities, the dashed one the vacancy component of Si self diffusivities and the dotted one the interstitialcy component of Si self diffusivities. Symbols are the experimental data from literature [6, 7, 12, 20-41]. The symbols in the rectangle [12, 37-41] are interstitialcy component of Si self diffusivities.

The literature data available for self diffusivities of Ge briefly reviewed in

section 3.2 are in good agreement. A single Arrhenius equation was utilized to fitting the selected diffusion coefficients measured using single crystalline Ge, as vacancy mechanism dominate the whole temperature range. The obtained equation for Ge self diffusivities is shown as:

$$D_{Ge}^T = 0.00777191 \exp\left(\frac{-310422.75}{RT}\right) \text{ m}^2/\text{s} \quad (10)$$

Hence, the activation energy for self diffusion of Ge is 3.22 eV due to the present evaluation. A comparison of the calculated diffusion coefficients and the measured ones is demonstrated in **Fig. 3**. It can be seen from the figure that a single Arrhenius equation can describe most of the experimental diffusivities well.

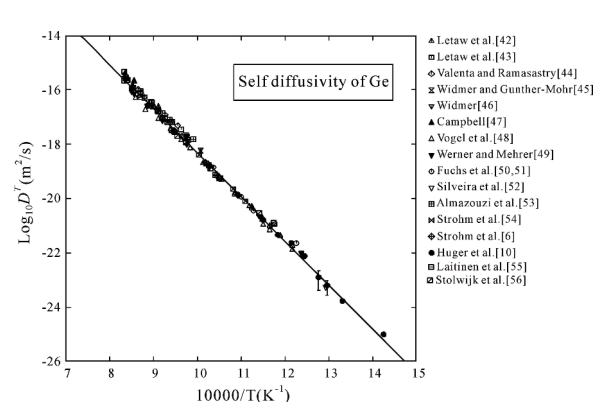


Figure 3. Self diffusivities of Ge. The symbols are the reported diffusivities in the literature, while the solid line is calculated according to the present atomic mobility parameters [6, 10, 42-56].

Similarly, the diffusivities of Si in Ge and those of Ge in Si were evaluated by the corresponding experimental data. When evaluating the impurity diffusivities of Si in Ge, only the experimental data from Sodervall and Friesel [66], Strohm et al. [6],

Lockwood et al. [62], Uppal et al. [67] and Silverstri et al. [11, 68] were utilized. That is because the data from Räsänen et al. [65] were measured in doped Ge samples. For the Ge diffusivities in Si, the data from Petrov et al. [57] were in polycrystalline Si and those from Lockwood et al. [62] show divergence with other data. Thus, those data [57, 62] were excluded from the parameter determination procedure. Due to the fact that there are not enough low temperature data, it is impossible to evaluate the vacancy component for Ge diffusion in Si. As a result only single Arrhenius was used. The obtained single exponentials are:

$$D_{Si\ in\ Ge}^T = 0.00314696 \exp\left(\frac{-319953.99}{RT}\right) \text{m}^2/\text{s} \quad (11)$$

$$D_{Ge\ in\ Si}^T = 0.44947087 \exp\left(\frac{-478685.86}{RT}\right) \text{m}^2/\text{s} \quad (12)$$

The comparison between the measured and the evaluated diffusivities of Si in Ge and those Ge in Si are presented in Fig. 4 and Fig. 5 respectively.

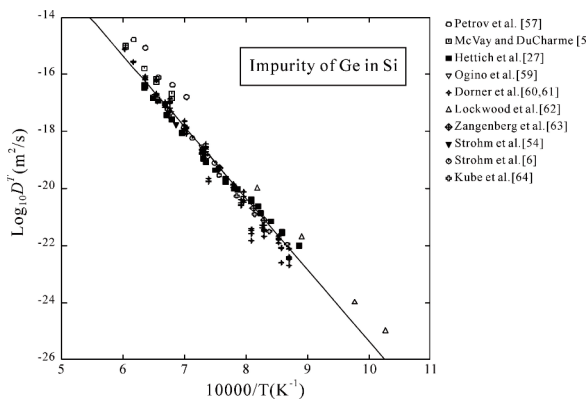


Figure 4. Impurity diffusivities of Ge in Si. The symbols are the reported diffusivities in the literature [6, 27, 54, 57-64], while the solid line is calculated according to the present atomic mobility parameters.

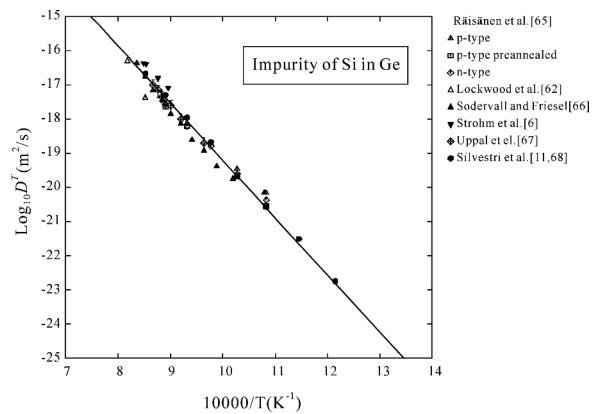


Figure 5. Impurity diffusivities of Si in Ge. The symbols are the reported diffusivities in the literature [6, 11, 62, 65-68], while the solid line is calculated according to the present atomic mobility parameters.

Thereafter, the interaction parameters in Eq. 7 were assessed from the tracer diffusivities of Si and Ge in the Ge-Si alloys. The tracer diffusivities of Ge measured by McVay and DuCharme [69] are not consistent with the data from others [6, 54, 55, 63, 64], and were thus excluded from the assessment. Besides, the tracer diffusivities measured by Zangenberg et al. [63] show divergence with the data measured by Strohm et al. [6, 54] at the concentrations  $x(\text{Ge}) = 0.3, 0.4$  and  $0.5$ . In the present assessment, the authors tend to trust the more systematical investigations by Strohm et al. [6, 54]. While the tracer diffusivities of Si [6, 55, 64] generally agree with each other. The finally obtained atomic mobility parameters are listed in Table 5. Figs. 6 and 7 are the model-predicted tracer diffusivities of Ge in comparison with the corresponding experimental data from Laitinen et al. [55], Strohm et al. [6, 54], Kube et al. [64] and Zangenberg et al. [63]. Meanwhile, the calculated tracer diffusivities of Si are

presented in **Fig. 8**. The experimental diffusivities from Strohm et al. [6], Laitinen et al. [55] and Kube et al. [64] are also appended for comparison. It is manifest that the presently obtained atomic mobility parameters can predict the experimental tracer diffusivities reasonably.

The interdiffusivities available in the literature are not consistent with each other. The data from Prokes and Spaepen [70] were measured in amorphous SiGe alloys. Whereas the interdiffusivities measured by Gavelle et al. [73, 74] exhibit wrong feature at  $x(\text{Si}) = 0$  to 0.7 and apparently disobey the

Table 5 The finally obtained atomic mobility parameters of diamond-structured Ge-Si alloys in the present work

Mobility	Parameters (in J/mole)	Reference
Si	$\Delta G_{\text{Si}}^{\text{Si}} = RT \ln(0.37146 \exp(\frac{-485572.27}{RT}) + 2.54332 \times 10^{-7} \exp(\frac{-345475.76}{RT}))$ $\Delta G_{\text{Si}}^{\text{Ge}} = -319953.99 - 47.90 \times T$ ${}^0 \Delta G_{\text{Si}}^{\text{Ge,Si}} = -259608.12 + 196.63 \times T$ ${}^1 \Delta G_{\text{Si}}^{\text{Ge,Si}} = +102337.32$	This work
Ge	$\Delta G_{\text{Ge}}^{\text{Si}} = -478685.86 - 6.65 \times T$ $\Delta G_{\text{Ge}}^{\text{Ge}} = -310422.75 - 40.38 \times T$ ${}^0 \Delta G_{\text{Ge}}^{\text{Ge,Si}} = +102336.83 - 109.61 \times T$ ${}^1 \Delta G_{\text{Ge}}^{\text{Ge,Si}} = -31761.55 + 33.54 \times T$	

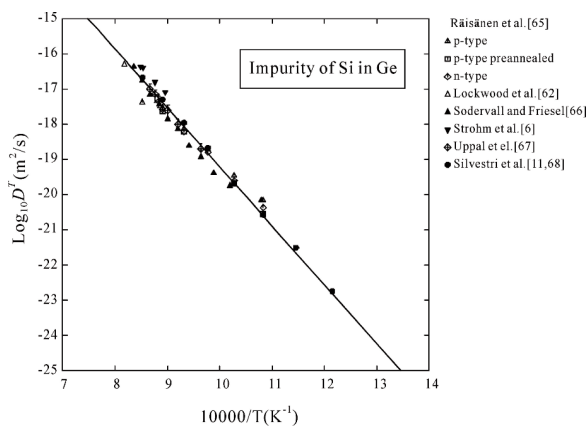


Figure 5. Impurity diffusivities of Si in Ge. The symbols are the reported diffusivities in the literature [6, 11, 62, 65-68], while the solid line is calculated according to the present atomic mobility parameters.

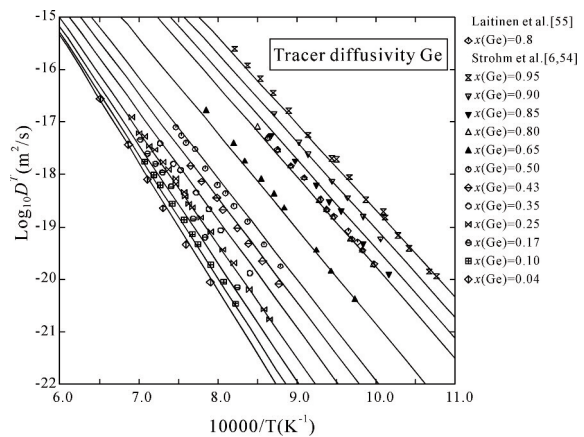


Figure 6. Model-predicted temperature dependence of tracer diffusivities of Ge in different Ge-Si alloys with diamond structure in comparison with the experimental data from Laitinen et al. [55] and Strohm et al. [6, 54].

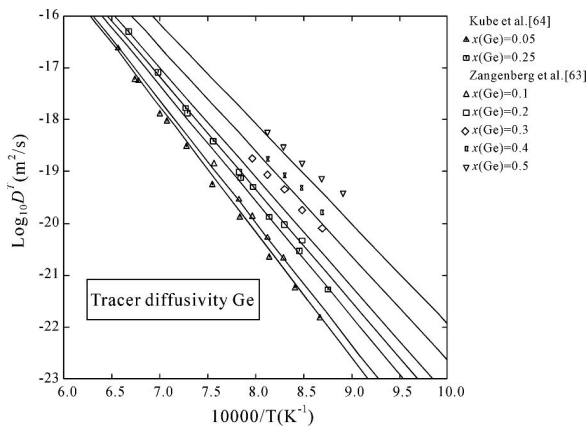


Figure 7. Model-predicted temperature dependence of tracer diffusivities of Ge in different Ge-Si alloys in comparison with the experimental data from Kube et al. [64] and Zangenberg et al. [63].

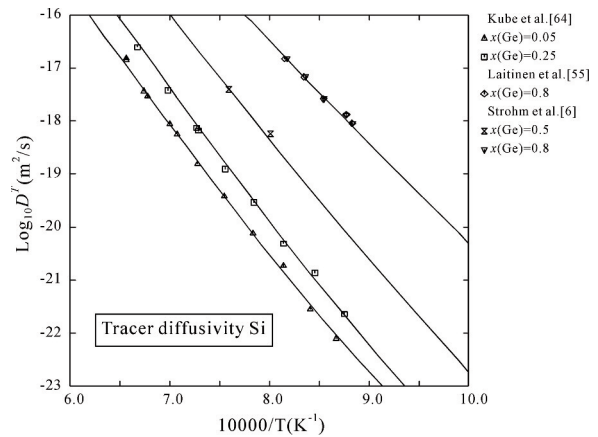


Figure 8. Model-predicted temperature dependence of tracer diffusivities of Si in different Ge-Si alloys in comparison with the experimental data from Kube et al. [64], Laitinen et al. [55], and Strohm et al. [6].

geometric relation,  $x(\text{Si}) \rightarrow 0$ ,  $\tilde{D} = D_{\text{Si in Ge}}^T$ . In addition, the data measured by Holländer et al. [72] at high Ge content  $x(\text{Ge})=0.46$  and  $0.68$  do not agree with those measured by Meduňa et al. [78-80]. Other experimental interdiffusivities [71, 75, 78-81] are generally in agreement with each other.

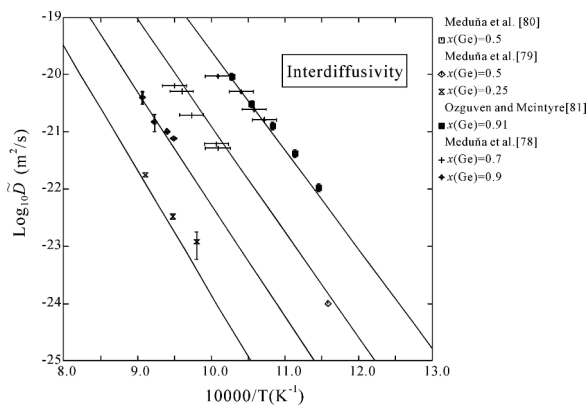


Figure 9. Model-predicted temperature dependence of interdiffusivities in different Ge-Si alloys in comparison with the experimental ones measured by Meduňa et al. [78-80] and Ozguven et al. [81].

Comparisons between the model-predicted and experimentally measured interdiffusivities are presented in **Figs. 9-12**. **Fig. 9** presented the model predicted temperature dependence of interdiffusivities together with the experimentally measured ones [78-81]. **Fig. 10** is the model-predicted composition dependence of interdiffusivities in comparison with the experimental ones

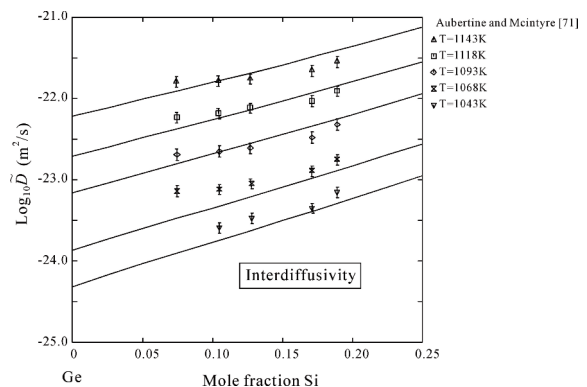


Figure 10. Model-predicted composition dependence of interdiffusivities in different Ge-Si alloys in comparison with the experimentally-measured ones by Aubertine and McIntyre [71].



obtained by Aubertine and McIntyre [71]. Similarly, **Fig. 11** demonstrates the calculated interdiffusion coefficients over the whole composition range of 1023-1173 K. The corresponding experimental ones were obtained by Gavelle et al. [73, 74]. While a comparison between the model-predicted and the measured interdiffusion

coefficients from Xia et al. [75-77] are shown in **Fig. 12**. From these figures, we can conclude that the presently obtained atomic mobilities can predict most of the reliable experimental data reasonably.

## 5. Simulations

### 5.1 Validation of the Manning theory in Ge-Si alloys

It is well known that the Darken relations that correlate the tracer diffusivities with intrinsic and interdiffusivities diffusivities are not complete if considering irreversible thermodynamics. Previous tests [85-87] in fcc structures indicated that the Manning's correction to the Darken relation in intrinsic diffusion coefficients is not significant in most systems within the realm of experimental error. However, the Darken-Manning relation in diamond structure is still not tested as far as the knowledge of the present authors. So we tend to examine the Manning correction to the Darken relation in diamond structure. Here we chose 1118 K as the testing temperature. Firstly, the composition dependence of the thermodynamic factor was determined by utilizing the thermodynamic description from Bergman et al. [82]. As presented in **Fig. 13**, the thermodynamic factor is symmetrical for the Ge-Si alloys at 1118 K and in the range of 0.8 ~ 1.0 over the whole composition range. Secondly, the 'vacancy wind term' and the vacancy wind factor were calculated by using the atomic mobility parameters obtained in section 4. It can be seen from **Fig. 14** that the 'vacancy wind term' for Ge ranges from 1 to 2. According to

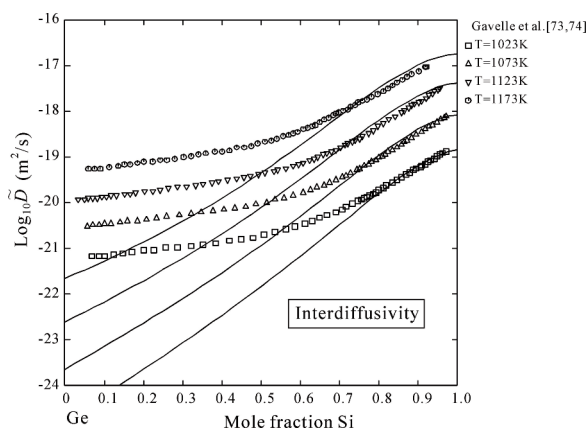


Figure 11. Model-predicted composition dependence of interdiffusivities in Ge-Si alloys at 1023-1173 K in comparison with the experimentally-measured ones by Gavelle et al. [73, 74].

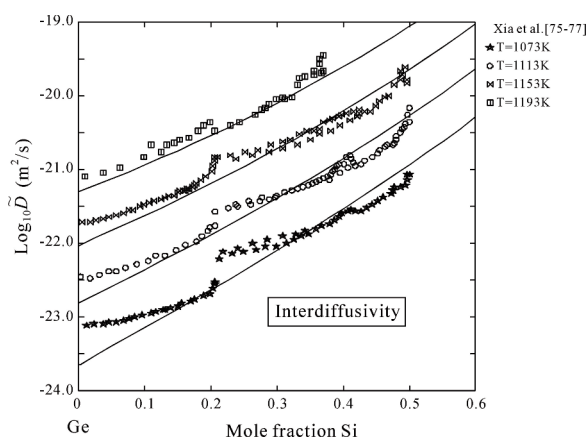


Figure 12. Model-predicted composition dependence of interdiffusivities in Ge-Si alloys at 1073, 1113, 1153 and 1193 K in comparison with the experimental ones from Xia et al. [75-77].

Eq. 2, this factor will enhance the intrinsic diffusion coefficient of Ge and even about 2 times for Ge rich alloys. It may be partially due to the fact that the  $M_o$  is 2 for diamond structure which is quite small in comparison with 7.15 for fcc structure. Meanwhile, the vacancy wind term for Si changes substantially from -0.5 to 1 indicating that it will slow the intrinsic diffusivities of Si and even change its sign. The vacancy wind factor varies between 1 and 1.5 and will enhance the interdiffusivities overall. **Fig. 15** presents the calculated intrinsic diffusivities and interdiffusivities at 1118 K by both Darken relation and Manning relation. As there is no report of intrinsic diffusivities in Ge-Si alloys, we could not conduct direct comparison for intrinsic diffusivities. Besides, even though there are experimental interdiffusivities at 1118 K, both Darken and Manning relation could not accurately predict the interdiffusivities as the data are much scatter (see the enlarged part of **Fig. 15**). But from the calculation result, the

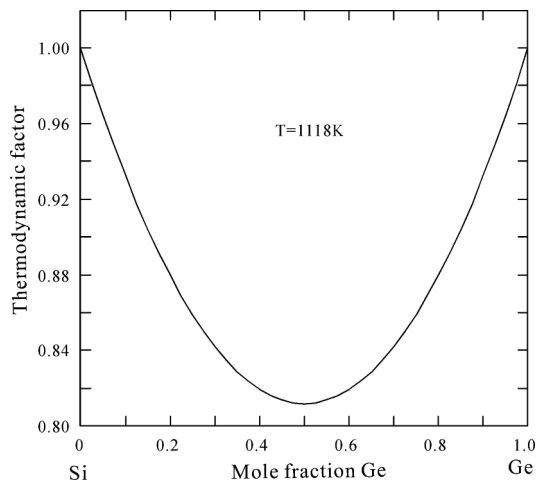


Figure 13. Calculated thermodynamic factor for Ge-Si alloys with diamond structure at 1118 K according to the thermodynamic parameters from Bergman et al. [82]

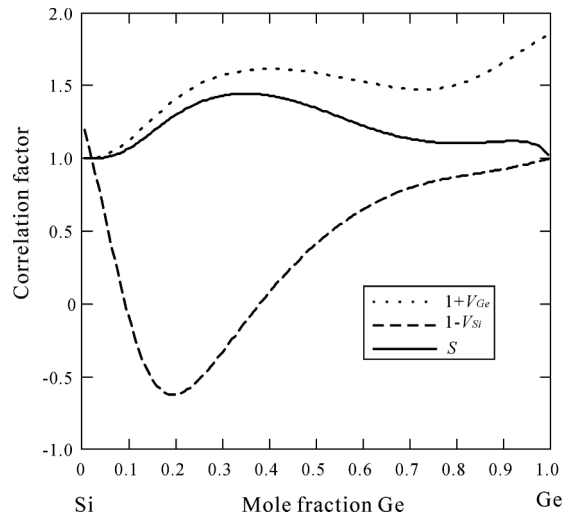


Figure 14. Calculated correlation factors for Ge-Si alloys at 1118 K. The dotted line is the 'vacancy wind term' for Ge, the dashed one the 'vacancy wind term' for Si, while the solid one the vacancy wind factor for Ge-Si alloys.

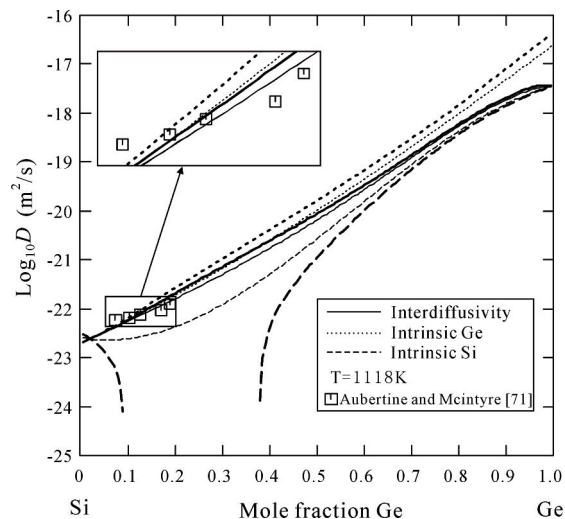


Figure 15. Model-predicted intrinsic diffusivities of Si and Ge as well as the model-predicted interdiffusivities at 1118 K according to different relations. The thick lines are from Manning relation, while the thin lines from Darken relation. The dashed lines are intrinsic diffusivities of Si, the dotted lines intrinsic diffusivities of Ge, while the solid lines interdiffusivities.

Manning modification will enhance the faster component and retard the slower component during the whole diffusion process. And the Manning modification even will change the sign of Si intrinsic diffusivities.

### 5.2 Simulation of diffusion in Ge-Si layers

Several Ge-Si diffusion couples were simulated in order to verify the reliability of the presently obtained atomic mobility parameters. **Fig. 16** is the model-predicted concentration profiles of a Si/Ge solid-solid diffusion couple at 1023 K for 10800 s, 36000 s, and 108000 s. The experimental data from Gavelle et al. [73, 74] are also appended for comparison. Similarly, the simulation results at 1173 K for about 600 s and 1800 s are presented in **Fig. 17** together with the corresponding experimental data [73, 74]. It is manifest from the results that the presently obtained atomic mobility parameter can accurately predict

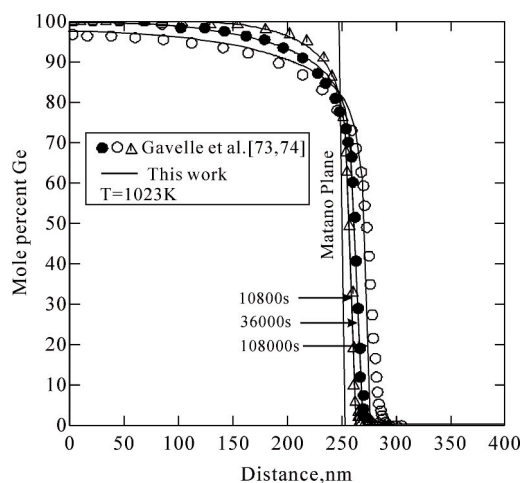


Figure 16. Model-predicted concentration profiles of Ge/Si thin layer diffusion couples annealed at 1023 K in comparison with the experimental data from Gavelle et al. [73, 74].

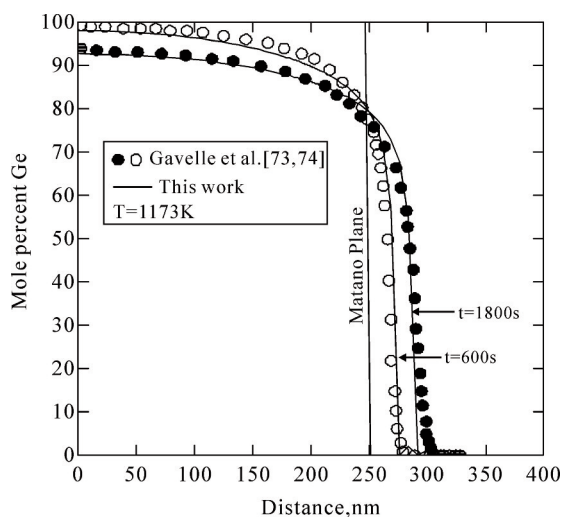


Figure 17. Model-predicted concentration profiles of Ge/Si thin layer diffusion couples annealed at 1173 K in comparison with the experimental data from Gavelle et al. [73, 74]

concentration profiles of these diffusion couples. The mobility parameters are capable of simulating the diffusion process in micro-scale and short annealing time. In details, there exist certain divergences between the simulated and the experimental concentration profiles. It may be due to the fact that thermodynamic parameters [82] are not accurate enough. In addition, experimental result [73, 74] may also have certain inaccuracy as the concentration is measured in micro-scale diffusion couples.

## 6. Conclusions

Various diffusivities (self-, tracer, impurity and chemical diffusivities) in Ge-Si alloys available in the literature were critically reviewed. The diffusion parameters for Si self diffusivities, Ge self diffusivities, impurity diffusivities of Si in Ge and Ge in Si were evaluated based on the selected

experimental information. For Si self diffusivities, the vacancy component and interstitialcy component are separated.

The Darken-Manning relation was tested in the diamond structure for the first time at 1118 K in the Ge-Si alloys. The calculated correlation factors are considerably large than those in fcc structure. The Manning's correction will retard the intrinsic diffusivities of Si, while enhance the intrinsic diffusivities of Ge and interdiffusivities.

The atomic mobility parameters for Ge-Si solid phase were determined by means of DICTRA assessment. The presently obtained atomic mobility parameters were then utilized to predict the concentration profiles of Ge-Si diffusion couples. The simulated results indicate that the obtained atomic mobility parameters are reliable. Thus, the presently obtained atomic mobility in diamond Ge-Si alloys can be utilized to construct atomic mobility database for semiconductors

### Acknowledgements

*The financial support from the National Natural Science Foundation of China (Grant Nos. 50721003 and 50831007), and National Basic Research Program of China (2011CB610401) is acknowledged. Lijun Zhang would like to thank the Alexander von Humboldt Foundation of Germany for supporting and sponsoring the research work at ICAMS, Ruhr-Universität Bochum, Germany.*

### References

- [1] D.J. Paul, Semicond. Sci. Technol. 19 (2004) R75.
- [2] X. Chen, Z. Wang, Y. Ma, J. Phys. Chem. C (2011) ACS ASAP.
- [3] D. Leonhardt, S.M. Han, Appl. Phys. Lett. 99 (2011) 111911/1.
- [4] B. Hu, Y. Du, H. Xu, W. Sun, W.W. Zhang, D. Zhao, J. Min. Metall. Sect. B-Metall. 46 (1) B (2010) 97.
- [5] Y. Du, J. Wang, Y.F. Ouyang, L.J. Zhang, Z.H. Yuan, S.H. Liu, P. Nash, J. Min. Metall. Sect. B-Metall. 46(1) B (2010) 1.
- [6] A. Strohm, T. Voss, W. Frank, P. Laitinen, J. Raisanen, Z. Metallkd. 93 (2002) 737.
- [7] Y. Shimizu, M. Uematsu, K.M. Itoh, Phys. Rev. Lett., 98 (2007) 095901/1.
- [8] L. Zhang, Y. Du, Y. Ouyang, H. Xu, X.G. Lu, Y. Liu, Y. Kong, J. Wang, Acta Mater. 56 (2008) 3940.
- [9] K. Tang, E. J. Oevrelid, G. Tranell, M. Tangstad, JOM. 61 (2009) 49.
- [10] E. Hüger, U. Tietze, D. Lott, H. Bracht, D. Bougeard, E.E. Haller, H. Schmidt, Appl. Phys. Lett. 93 (2008) 162104/1.
- [11] H.H. Silvestri, H. Bracht, J.L. Hansen, A.N. Larsen, E. E. Haller, Semicond. Sci. Technol. 21 (2006) 758.
- [12] H. Bracht, N.A. Stolwijk, H. Mehrer, Phys. Rev. B 52 (1995) 16542.
- [13] K. Compaan, Y. Haven, Trans. Faraday Soc. 52 (1956) 786.
- [14] M. Posselt, F. Gao, H. Bracht, Phys.

- Rev. B 78 (2008) 035208.
- [15] K. Compaan, Y. Haven, *Trans. Faraday Soc.*, 52 (1958) 1498.
- [16] J.R. Manning, *Metall. Trans*, 1 (1970) 499.
- [17] J.O. Andersson, J. Ågren, *J. Appl. Phys.* 72 (1992) 1350.
- [18] J.O. Andersson, T. Helander, L. Höglund, P. Shi, B. Sundman, *CALPHAD* 26 (2002) 273.
- [19] O. Redlich, A.T. Kister, *J. Ind. Eng. Chem. (Washington, D. C.)* 40 (1948) 84.
- [20] B.J. Masters, J.M. Fairfield, *Appl. Phys. Lett.* 8 (1966) 280.
- [21] R.N. Ghoshtagore, *Phys. Rev. Lett.* 16 (1966) 890.
- [22] R.F. Peart, *Phys. Status Solidi* 15 (1966) K119.
- [23] J.M. Fairfield, B.J. Masters, *J. Appl. Phys.* 38 (1967) 3148.
- [24] I.R.D. Sanders, P.S. Dobson., *J. Mater.Sci.* 9, (1974) 1987.
- [25] H.J. Mayer, H. Mehrer, K. Maier, *Inst. Phys. Conf. Ser.* 31 (1977) 186.
- [26] J. Hirvonen, A. Anttila, *Appl. Phys. Lett.* 35 (1979) 703.
- [27] G. Hettich, H. Mehrer, K. Maier, *Conf. Ser. - Inst. Phys.* 46 (1979) 500.
- [28] L. Kalinowski, R. Seguin, *Appl. Phys. Lett.* 35 (1979) 211.
- [29] F.J. Demond, S. Kalbitzer, H. Mannsperger, H. Damjantschitsch, *Phys. Lett.* 93A (1983) 503.
- [30] H. Bracht, E.E. Haller, K. Eberl, M. Cardona, R. Clark-Phelps, *Mater. Res. Soc. Symp. Proc.* 527 (1998) 335.
- [31] A. Ural, P.B. Griffin, J.D. Plummer, *Appl. Phys. Lett.* 79 (2001) 4328.
- [32] A. Ural, P.B. Griffin, J.D. Plummer, *Phys. Rev. Lett.* 83 (1999) 3454.
- [33] Y. Nakabayashi, H.I. Osman, T. Segawa, K. Saito, S. Matsumoto, J. Murota, K. Wada, T. Abe, *Jpn. J. Appl. Phys. Part 2* 40 (2001) L181.
- [34] Y. Nakabayashi, H.I. Osman, K. Toyonaga, K. Yokota, S. Matsumoto, J. Murota, K. Wada, T. Abe, *Jpn. J. Appl. Phys. Part 1* 42 (2003) 3304.
- [35] S.R. Aid, T. Sakaguchi, K. Toyonaga, Y. Nakabayashi, S. Matsumoto, M. Sakuraba, Y. Shimamune, Y. Hashiba, J. Murota, K. Wada, T. Abe, *Mater. Sci. Eng. B* B114-B115 (2004) 330.
- [36] Y. Shimizu, K. M. Itoh, *AIP Conf. Proc.* 893 (2007) 205.
- [37] N.A. Stolwijk, B. Schuster, J. Hoelzl, *Appl. Phys. A* A33 (1984) 133.
- [38] S. Mantovani, C. N. F. Nava, G. Ottaviani, *Phy. Rev. B* 33, (1986) 5536.
- [39] M. Perrett, N.A. Stolwijk, L. Cohauszss, *J. Phys.: Condens. Matter* 1 (1989) 6347.
- [40] D. Grünebaum, Th. Czekalla, N.A. Stolwijk, H. Mehrer, I. Yonenaga, K. Sumino, *Appl. Phys. A* 53 (1991) 65.
- [41] J. Hauber, W. Frank, N.A. Stolwijk, *Mater. Sci. Forum* 38-41 (1989) 707.
- [42] H. Letaw, W.M. Portnoy, L. Slifkin, *Phys. Rev.* 102 (1956) 636.

- [43] H. Letaw, L.M. Slifkin, W. M. Portnoy, Phys. Rev. 93 (1954) 892.
- [44] M.W. Valenta, C. Ramasastry, Phys. Rev. B 106 (1957) 73.
- [45] H. Widmer, G. R. Gunther-Mohr, Helv. Phys. Acta 34 (1961) 635.
- [46] H. Widmer, Phys. Rev. 125 (1962) 30.
- [47] D.R. Campbell, Phys. Rev. B 12 (1975) 2318.
- [48] G. Vogel, G. Hettich, H. Mehrer, J. Phys. C 16 (1983) 6197.
- [49] M. Werner, H. Mehrer, H.D. Hochheimer, Phys. Rev. B 32 (1985) 3930.
- [50] H.D. Fuchs, W. Walukiewicz, E.E. Haller, W. dondl, R. Schorer, and G. Abstreiter, Phys. Rev. B 51 (1995) 16817.
- [51] E.E. Haller, L. Wang, Diffus. Defect Data, Pt. A 143-147 (1997) 1067.
- [52] E. Silveira, W. Dondl, G. Abstreiter, E.E. Haller, Phys. Rev. B 56 (1997) 2062.
- [53] A. Almazouzi, E.G. Moya, J. Bernardini, Defect and Diffusion Forum 143-147 (1997) 1047.
- [54] A. Strohm, T. Voss, W. Frank, J. Raisanen, M. Dietrich, Physica B (Amsterdam, Neth.) 308-310, (2001) 542.
- [55] P. Laitinen, A. Strohm, J. Huikari, A. Nieminen, T. Voss, C. Grodon, I. Riihimaki, M. Kummer, J. Aysto, P. Dendooven, J. Raisanen, W. Frank, Phys. Rev. Lett. 89 (2002) 085902/1.
- [56] N.A. Stolwijk, W. Frank, J. Hblzl, S.J. Pearton, E.E. Haller, J. Appl. Phys. 57 (1984) 5212.
- [57] D.A. Petrov, Y.M. Shashkov, I.P. Akimchenko, Voprosy Met. i Fiz. Poluprovodnikov (Moscow: Akad. Nauk S.S.S.R.) Sbornik (1957) 130.
- [58] G.L. McVay, A.R. DuCharme, J. Appl. Phys. 44 (1973) 1409.
- [59] M. Ogino, Y. Oana, M. Watanabe, Phys. Status Solidi A 72 (1982) 535.
- [60] P. Dorner, W. Gust, A. Lodding, H. Odelius, B. Predel, U. Roll, Diffus. Defect Monogr. Ser. 7 (1983) 488.
- [61] P. Dorner, W. Gust, B. Predel, U. Roll, A. Lodding, H. Odelius, Philos. Mag. A 49 (1984) 557.
- [62] D.J. Lockwood, J.M. Baribeau, H.J. Labbe, Can. J. Phys. 70 (1992) 852.
- [63] N.R. Zangenberg, J. Lundsgaard Hansen, J. Fage-Pedersen, A. Nylandsted Larsen, Phys. Rev. Lett. 87 (2001) 125901.
- [64] R. Kube, H. Bracht, J. Lundsgaard Hansen, A. Nylandsted Larsen, E.E. Haller, S. Paul, W. Lerch, Mater. Sci. Semicond. Process. 11 (2008) 378.
- [65] J. Räisänen, J. Hirvonen, A. Anttila, Solid-State Electron. 24 (1981) 333.
- [66] U. Sodervall, M. Friesel, Defect and Diffusion Forum 143-147 (1997) 1053.
- [67] S. Uppal, A.F. W. Willoughby, J.M. Bonar, N.E.B. Cowern, R.J.H. Morris, M.G. Dowsett, Mater. Res. Soc. Symp. Proc. 809 (2004) 237.
- [68] H.H. Silverstri, H. Bracht, J.L. Hansen, A.N. Larsen, E.E. Haller, AIP Conf. Proc. 772 (2005) 97.
- [69] G.L. McVay, A.R. DuCharme, Phys. Rev. B 9 (1974) 627.

- [70] S.M. Prokes, F. Spaepen, *Appl. Phys. Lett.* 3 (1985) 234.
- [71] D.B. Aubertine, P.C. McIntyre, *J. Appl. Phys.* 97 (2005) 013531/1.
- [72] B. Hollander, R. Butz, S. Mantl, *Phy. Rev. B* 64 (1992) 6975.
- [73] M. Gavelle, E.M. Bazizi, E. Scheid, C. Armand, P.F. Fazzini, M. Olivier, Y. Campbell, A. Halimaoui, F. Cristiano, *Mater. Sci. Eng. B* 154-155 (2008) 110.
- [74] M. Gavelle, E.M. Bazizi, E. Scheid, P.F. Fazzini, F. Cristiano, C. Armand, W. Lerch, S. Paul, Y. Campidelli, A. Halimaoui, *J. Appl. Phys.* 104 (2008) 113524/1.
- [75] G. Xia, M. Canonico, J.L. Hoyt, *Semicond. Sci. Technol.* 22 (2007) S55.
- [76] G. M. Xia and J. L. Hoyt, *J. Appl. Phys.* 101 (2007) 044901.
- [77] G. Xia, O.O. Olubuyide, J.L. Hoyt, *Appl. Phys. Lett.* 88 (2006) 013507.
- [78] M. Meduňa, O. Caha, M. Keplinger, J. Stangl, G. Bauer, G. Mussler, D. Grutzmacher, *Phys. Status Solidi A* 206 (2009) 1775.
- [79] M. Meduňa, J. Novak, G. Bauer, C.V. Falub, D. Grutzmacher, *Phys. Status Solidi* 205 (2008) 2441.
- [80] M. Meduňa, J. Novak, G. Bauer, V. Holy, C. V. Faulb, S. Tsujino, D. Grutzmacher, *Semicond. Sci. Technol.* 22 (2007) 447.
- [81] N. Ozguven, P.C. McIntyre, *Appl. Phys. Lett.* 92 (2008) 181907/1.
- [82] C. Bergman, R. Chastet, R. Castanet, *J. Phase Equilib.* 13 113 (1992).
- [83] H.M. Morrison, *Phil. Mag.* 31 (1975) 243.
- [84] M.M. De Souza, E.M. Sankara Narayanan, *Defect and Diffusion Forum* 153-155 (1998) 69.
- [85] F.J.J.v. Loo, *Progress in Solid State Chemistry* 20 (1990) 47.
- [86] M.J.H. van Dal, M.C.L.P. Pleumeekers, A.A. Kodentsov, F.J.J.v. Loo, *J. Alloys Compd.* 309 (2000) 132.
- [87] N.S. Kulkarni, PhD thesis, University of Florida (2004).